Shap. Mem. Superelasticity (2023) 9:116–126
https://doi.org/10.1007/s40830-023-00430-4

TECHNICAL ARTICLE

Viewpoint: Tuning the Martensitic Transformation Mode in Shape Memory Ceramics via Mesostructure and Microstructure Design

Donald J. Erb[1] · Hunter A. Rauch[1] · Kendall P. Knight[1] · Hang Z. Yu[1]

Received: 30 November 2022 / Revised: 23 February 2023 / Accepted: 6 March 2023 / Published online: 24 March 2023

Abstract The shape memory and superelastic effects are based on mechanically or thermally induced martensitic transformation. In bulk monolithic shape memory materials, these effects are characterized by a driving force threshold, such as a critical stress or a critical temperature, above which the transformation is completed within a relatively narrow window of stress or temperature. In this viewpoint article, we discuss the tuning of macroscopic martensitic transformation characteristics via mesostructure and microstructure design: with heterogeneous driving force and low nucleation barrier in meso-/micro-structured shape memory materials, especially shape memory ceramics, local transformation events can occur sequentially rather than simultaneously. This can lead to a globally continuous transformation mode without well-defined critical stress or temperature. Based on the insights from mechanics modeling and experimental evidence, we illustrate this effect in granular packings, metal matrix composites, and cellular architectures, and discuss how it may unlock new possibilities for applications involving actuation and energy dissipation.

Keywords Shape memory · Martensitic transformation · Zirconia · Granular materials · Mesostructure · Mechanical constraint

Introduction

Shape memory materials are those which can 'remember' an initial shape upon heating, even after undergoing apparently permanent plastic deformation. This is possible owing to detwinning of the martensite phase in the 'shape memory regime' ($T < M_f$) or irreversible martensitic transformation upon mechanical loading in the 'intermediate regime' ($M_s < T < A_s$) [1]. What appears to be plastic deformation is instead detwinning or transformation-mediated plasticity. The differences between the geometry of twinned and detwinned martensites or between the austenite and martensite crystal structures are responsible for the shape change. Heating the material above a critical temperature will trigger the reverse martensitic transformation; the original shape is recovered upon cooling to the initial temperature. This is the so-called shape memory effect. The same material can display the superelastic effect as well in the 'superelastic regime' ($T > A_f$), in which large recoverable strains arise as a result of reversible martensitic transformation upon mechanical loading and unloading [2]. The shape memory and superelastic effects have been studied in bulk metallic and ceramic materials for decades [3–11].

Beyond the conventional bulk form, recent advances in modeling and processing have allowed materials scientists to flex their creativity and explore structural and functional materials in new ways, especially through mesostructure engineering. Here, "meso-" means intermediate, in between macro- and micro- scales. In a broader sense,

This article is an invited submission to *Shape Memory and Superelasticity* selected from presentations at the Shape Memory and Superelastic Technology Conference and Exposition (SMST2022) held May 16–20, 2022 at The Westin Carlsbad Resort, San Diego, California and has been expanded from the original presentation. The issue was organized by Dr. Srinidhi Nagaraja, G.RAU, Inc. and Dr. Ashley Bucsek, University of Michigan.

✉ Hang Z. Yu
hangyu@vt.edu

[1] Department of Materials Science and Engineering, Virginia Tech, Blacksburg, VA 24061, USA

mesostructured materials are those with structural or compositional heterogeneities on the length scale in between the macroscopic shape and microstructure, including cellular architectured materials [12, 13], functionally graded materials [14], as well as composites and hybrid materials [15]. Through topological design and optimization [16–18] or fractal designs [19], mesostructured materials can be engineered for specific applications. For example, metallic honeycombs are demonstrated to have superior collision energy absorption performance [20], thin-walled aluminum oxide truss structures can elastically recover incredible strains [21], and piezoelectric-elastomer composites can harvest mechanical energy as electricity through bending [22]. Along with topology, the mesoscale feature size or characteristic length is another key factor in governing the macroscopic response of the material. If the feature size is sufficiently small, the size effect of an individual strut may play a role and result in unprecedentedly remarkable properties, as seen in nano-architectured materials [23, 24].

Applying the mesostructure engineering strategy while leveraging the traditional microstructure engineering wisdom can unlock new opportunities for material design, wherein the material response to external stimuli is robustly engineered and tailored for target applications [19, 25–29]. In the context of shape memory ceramics, this can change the characteristics of thermodynamic driving force and nucleation barrier in mechanically induced and thermally induced martensitic transformation. When a mesostructured shape memory ceramic is subjected to macroscopically uniform loading like uniaxial compression or tension, the highly heterogeneous stress distribution can lead to spatially non-uniform distribution of the transformed regions. When the mesoscale characteristic length scale, e.g., strut width for a cellular architectured material, particle size for a granular packing, or filament width for a composite, is comparable to the microscale characteristic length scale, which is mostly defined by the grain size, the mechanical constraint against deformation and martensitic transformation can be significantly reduced [30]. This can suppress phenomena commonly observed in bulk monolithic shape memory ceramics, such as autocatalysis. This is because the transformation-induced strain cannot be transferred on a larger scale to other particles in granular packings or composites, or other ligaments in cellular architectures.

In this viewpoint article, we discuss how coupled mesostructure and microstructure design can be used to tune the global transformation mode in shape memory ceramics. By matching the feature sizes on the meso- and microscale, the transformation volume can continuously change with the amplitude of external stimuli without an apparent critical stress or temperature. Such a globally 'continuous mode' is caused by sequential local transformation events, distinguishing itself from the threshold-based transformation behavior in bulk monolithic shape memory materials. This will unlock new opportunities for actuation and energy dissipation applications. Through simulations and experiments, we demonstrate this effect in granular packings, metal matrix composites, and cellular architectured materials. While the 'continuous mode' of transformation can also be realized through local composition modulation [31] or impurity doping [32], the strategy of microstructure and mesostructure engineering opens new paths for experimental implementation, e.g., through advanced materials processing and additive manufacturing.

Central Concept

For the stress-induced martensitic transformation in bulk monolithic shape memory materials starting with 100% austenite phase, the content of martensite typically remains zero until a critical stress is reached as shown in Fig. 1A. Full conversion of the austenite phase to martensite is accomplished over a narrow stress window, above which the material is fully martensite [8]. Fundamentally, this is a caused by two factors: (i) a relatively uniform stress distribution in the bulk material upon loading and (ii) strong intergranular mechanical constraint that results in restricted transformation characterized by self-accommodation and autocatalysis. A meso/micro-structured shape memory material, however, is designed to have a non-uniform stress state and weak mechanical constraint. This will lead to transformation behavior more like in Fig. 1B, where austenite can be converted to martensite even at relatively low loads due to high stress concentration and low nucleation barrier. While each sub-element would still have a critical stress for martensite nucleation, the overall heterogeneous stress means that only a fraction of material would experience stresses exceeding the critical level at a given load. Further, since the individual sub-elements are separated from one another in granular packings, composites, and cellular architectures, the martensite formation is nucleation-dominated and large-scale growth of the martensite cannot occur via autocatalysis. As the macroscopic load increases incrementally, more martensite is formed, resulting in sequential local transformation events.

For example, in a granular packing under a given loading condition, a fraction of the inter-particle contacts is above the critical stress, but a large fraction of eligible contacts are not; as the applied compressive load is increased, the average stress on a particle contact increases, and the fraction of particles experiencing critical stress also increases. This initial transformation gives the upward concavity shown in Fig. 1B. At higher applied loads, as the

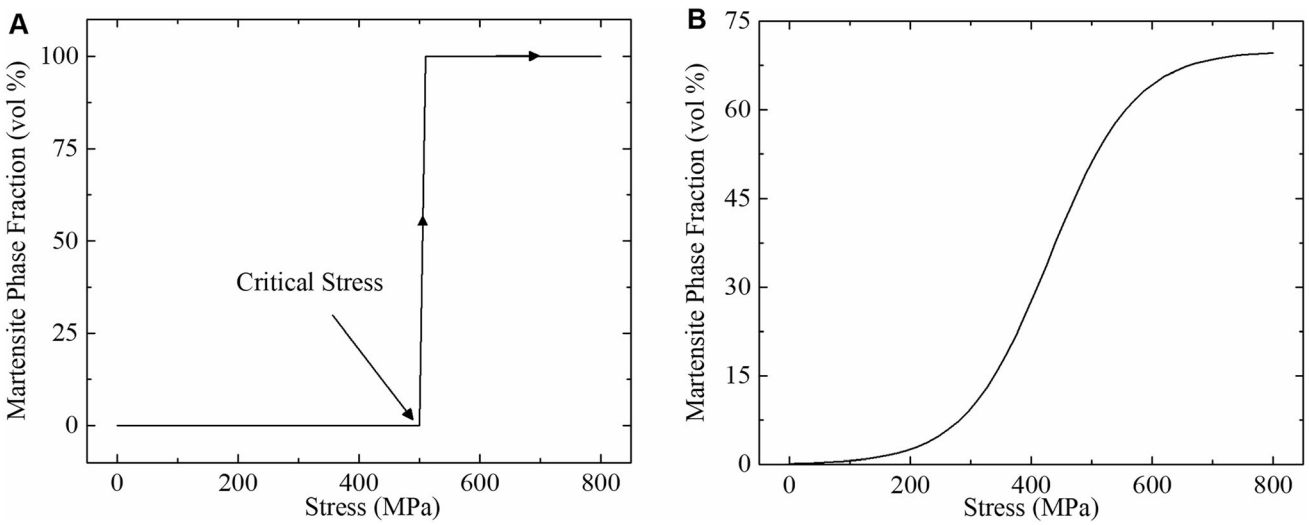

Fig. 1 Volume fraction of martensite from loading for **A** bulk monolithic and **B** meso/micro- engineered shape memory materials

austenite is converted to martensite at the areas of maximum stress, the martensitic phase then begins to bear more of the stress and prevents additional conversion of the austenite phase [1]. Thus, the rate of transformation as a function of stress will initially be high as the contact stresses increase, but then will reduce as less load is effectively transferred to regions with austenite, as illustrated in Fig. 1B. Overall, stress-induced martensitic transformation in a meso/micro-structured shape memory material can display a seemingly continuous transformation mode [1].

Figure 2 illustrates two such applications where the continuous transformation mode in meso/micro-engineered shape memory materials can exhibit better traits than their bulk counterparts. Figure 2A compares the energy absorption behavior of a panel of bulk shape memory material and its meso- or micro-structured counterpart that is characterized by non-uniform stress distribution and weak mechanical constraint. Using a material in its superelastic regime would allow energy absorption as the material is loaded, transforming from austenite to martensite, and unloaded, reverting the martensite back to austenite. The total absorbed energy is defined by the area of the hysteresis loop between loading and unloading. The bulk material requires the critical stress to be reached before any martensitic transformation could occur. Thus, if the panel is bombarded with particles of masses smaller than needed to exert the critical stress, then the panel will

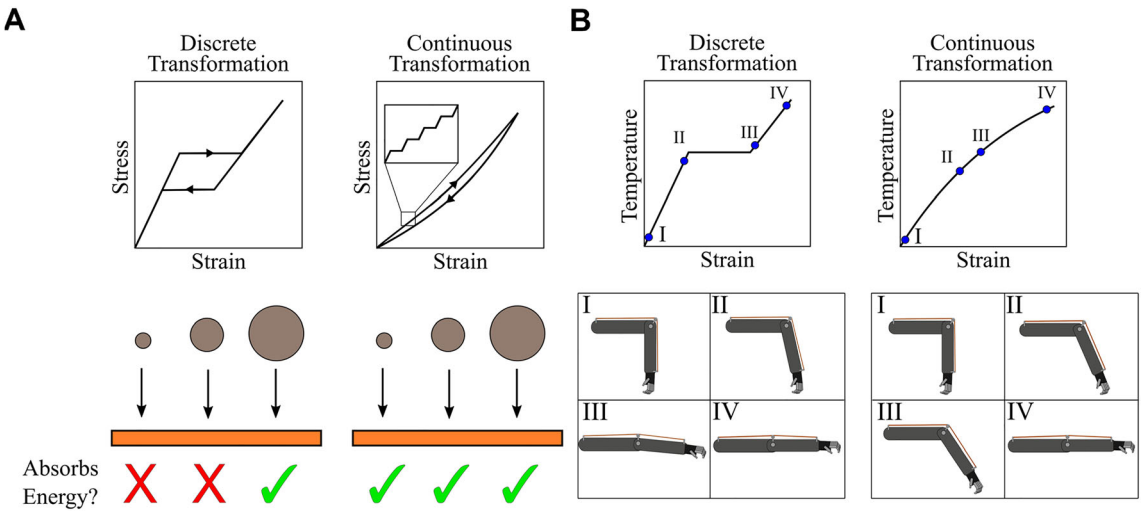

Fig. 2 Application differences between the discrete transformation exhibited by bulk shape memory materials and the continuous transformation of meso/micro-structured shape memory materials: **A** energy absorption where the continuous transformation allows for absorbing energy from multiple stress levels due to a lower effective critical stress for transformation and **B** actuation where the full range of motion is achievable since the transformation occurs over a broad temperature range

not absorb any of the energy outside of the conventional inelasticity of the impact. In contrast, a panel made from meso-/micro-structured shape memory material would exhibit a continuous transformation mode and thus can absorb energy from particles with a broad range of sizes or masses, resulting in a more universal energy dissipation capability.

For meso/micro-structured shape memory materials that have undergone irreversible stress-induced martensitic transformation, there will be a non-uniform distribution of the martensite phase upon load removal. Post-load heating then results in reverse martensitic transformation in previously partially transformed particles or ligaments. During heating, although the temperature is uniform in the material, the non-uniform initial martensite distribution can also lead to a continuous transformation mode because local regions with different values of A_s can transform more independently in the absence of strong mechanical constraint [33, 34]. This effect may be leveraged for robust control of actuation. Figure 2B displays the actuation of a mechanical arm using wires of shape memory material. For a bulk shape memory material, the arm will have a relatively discrete actuation as the temperature increases from A_s (point II) to A_f (point III). Due to this actuation behavior, the movement of the mechanical arm is not smooth; it is challenging for the arm to achieve a region of actuation between points II and III. In contrast, using a meso/micro-engineered shape memory material for the wire would enable continual actuation with heat and would thus allow for a smoother movement and a larger controllable range of motion.

From a material design perspective, what is the requirement for meso/micro-structured shape memory materials to display the globally continuous transformation mode? To promote heterogeneous stress distribution, mesoscale structural heterogeneity is a key; it is available in granular packings, cellular architectured materials, and composites and hybrid materials. To lower the nucleation barrier, mechanical constraint should be minimized. This can be achieved by increasing the free surface area via mesostructure engineering and by eliminating the triple junctions through matching the mesoscale and microscale characteristic lengths. This is especially important for shape memory ceramics such as ZrO_2 in which the transformation strain is larger than its elastic limit, so free surfaces are necessary to avoid fracture from the transformation [27]. For granular packings or composites consisting of shape memory particles in a matrix material, the intergranular constraint can be minimized using single-crystal particles. For cellular architectured materials, intergranular constraint can be minimized by forming a bamboo-like microstructure with the grain size equal to the strut width.

Figure 3 depicts the localized martensite nucleation with increasing applied stress for these micro- and meso-engineered structures: a granular packing, a composite, and a honeycomb structure. The granular packing consists of single-crystal shape memory particles as shown in Fig. 3A**.** The packing is expected to form martensite gradually due to the evolution of the force chains and weak inter-particle constraint [35, 36]. The composite contains single-crystal shape memory particles embedded in a matrix as shown in Fig. 3B**.** Having the particles acting as stress concentrators with zero intergranular mechanical constraint, local martensitic transformation can occur separately at lower stresses than the nominal critical stress, resulting in a continuous transformation mode. The meso/micro-engineered honeycomb structure in Fig. 3C is characterized by highly heterogeneous stress distribution upon axial compression. Owing to a lot of free surface area and the absence of triple junctions enabled by bamboo-like microstructures, the martensite plates would nucleate easily at stress concentration sites from loading. The main advantage of the meso/micro-engineered shape memory material is that it enables precise tuning of the martensite volume fraction as a function of the external loading by merely altering the structural arrangement on the two length scales.

Insights from Constitutive Modeling

Mechanics analysis and constitutive modeling can provide insights into the martensitic transformation behavior of the meso/micro-structured shape memory materials. The thermodynamical constitutive modeling for shape memory materials allows us to predict the martensite content as a function of macroscopic loading [37]. This treatment is not intended to simulate details of the austenite–martensite transformation, which depends on the stress state as well as microstructure and crystallography. Instead, we approach the problem from a perspective of state variables to approximate the transformed volume that might be achieved on average. Here, finite element analysis is implemented via COMSOL Multiphysics 5.6 using the Lagoudas model in the Nonlinear Structural Materials Module, which defines the Gibbs free energy of the system using stress and temperature as the state variables [38–41]. For the two models shown in Fig. 4, the following parameters are used to define stress-induced transformation: martensite start stress of 1050 MPa, martensite finish stress of 1350 MPa, austenite start stress of 600 MPa, and austenite finish stress of 200 MPa [8, 42, 43]. These numbers reflect the high critical stresses of ZrO_2-based shape memory ceramics. The depicted structures are fixed on the bottom face, while the top face is subjected to

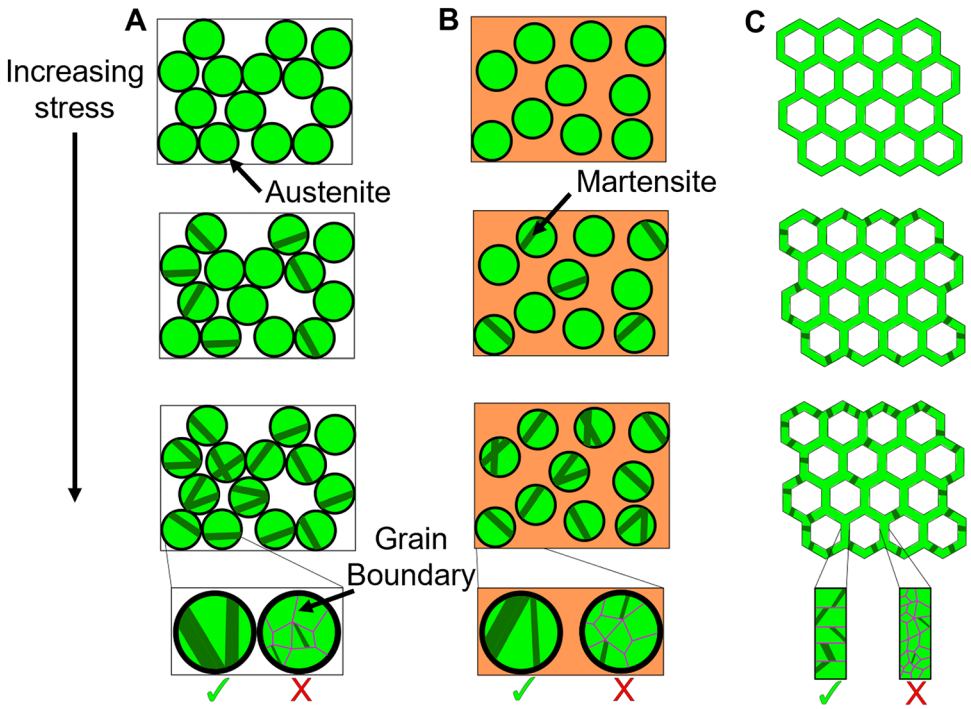

Fig. 3 Martensite formation from applied stress for **A** granular packings, **B** metal matrix composites, and **C** meso-engineered structures; for all scenarios, martensite forms due to heterogeneous stress concentrations. The bottom zoomed-in portions compare martensite formation in regions with low and high mechanical constraints, respectively, in which the lower mechanical constraints allow for further martensite nucleation

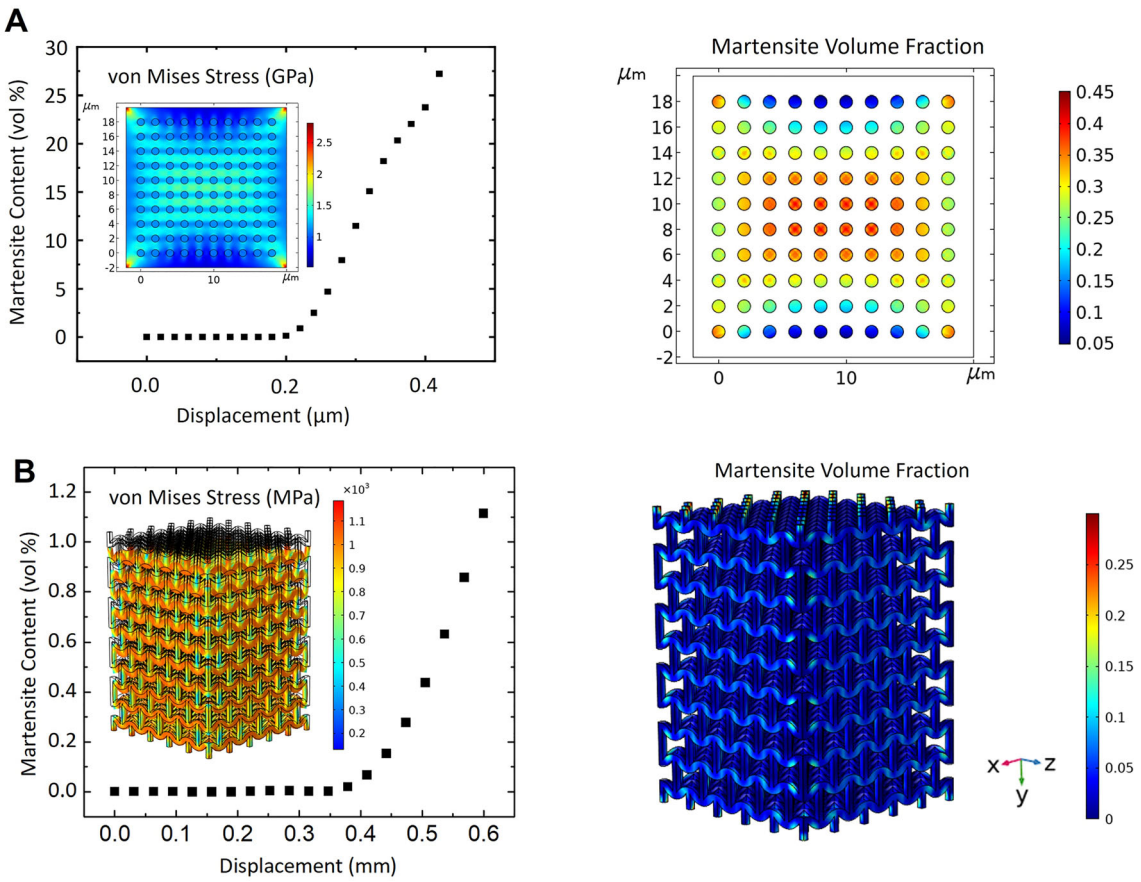

Fig. 4 Simulations of martensite content versus displacement during compression and the resulting local von Mises stress and martensite volume fraction for **A** ZrO_2 particles in an aluminum matrix and **B** a pure ZrO_2 meso-engineered structure

constant displacement, simulating a typical compression test. Each node within the model has a critical stress above which it transforms from austenite to martensite.

We first analyze a metal matrix composite, Al-22vol%ZrO_2, in which single-crystal shape memory ceramic ZrO_2 particles are embedded into the Al matrix. Here, ZrO_2 is doped with an appropriate amount of other oxides (e.g., 15-mol% CeO_2) to be in the superelastic regime. Figure 4A depicts a two-dimensional model of the composite 22 × 22 μm in size with the ZrO_2 particle size of 1 μm. The composite is subjected to compression with a displacement rate of 0.2 μm/s. Similar to the behavior of a bulk shape memory alloy illustrated in Fig. 1A, the composite has no martensite formation until a critical displacement; however, the martensite content then gradually increases with further displacement, more closely matching the behavior depicted in Fig. 1B. The gradual increase in martensite content is due to the heterogeneous stress experienced by the individual particles as depicted by the von Mises stresses at the maximum displacement in the inset of Fig. 4A. Likewise, the martensite content of the individual ZrO_2 particles shows a location dependence that is directly tied to the heterogeneous stress experienced during compression. By tuning the spatial, size, composition, and orientation distribution of ZrO_2 particles, changing the shape of the entire composite material, or changing the testing condition (i.e., temperature, hydrostatic pressure, and loading configuration and direction), the resulting macroscopic transformation behavior can be tuned robustly.

We next analyze the transformation behavior of a superelastic cellular micro-architectured material also based on shape memory ceramic ZrO_2. Figure 4B depicts a three-dimensional model of a meso/micro-engineered ZrO_2 structure consisting of 125 (5 × 5 × 5) repeated auxetic (negative Poisson ratio) truss structures—each 13.9 × 13.9 × 18.1 mm in size with vertical struts of 9 mm, re-entrant struts of 4.5 mm, re-entrant angles of 60°, and strut thicknesses of 1.6 mm [44]. During compression, the displacement rate is 2 mm/s. The martensite content during loading closely resembles the simulated metal matrix composite in Fig. 4A, with no martensite formation until a critical displacement, followed by a gradual increase as displacement increases. The martensite formation behavior is likewise due to the heterogeneous stress distribution within the structure, with larger von Mises stresses and local martensite contents at the joints of the structure. Stress concentration sites will first transform under load; the spatial distribution, orientation, and connectivity of the stress concentration sites are thus factors in governing the shape memory performance of the meso/micro-structured shape memory material.

In the above two examples based on shape memory ceramics, the continuous transformation mode is achieved but the critical stress or displacement does exist. This is because of the moderate level of mechanical constraint arising from the geometrical features of composites and architectured materials. If the mechanical constraint can be further reduced like that in a granular packing, the critical stress may no longer exist. In the literature, the transformation behavior of mesostructured shape memory alloy NiTi has been investigated [19], which is modeled as Menger sponge-like structures with different fractal dimensions using constitutive models based on Lagoudas [39–41] and Auricchio [45–47].

Experimental Evidence

While the central concept of tuning the transformation mode via meso/micro-structure design has been demonstrated in mechanics modeling, it is desirable to prove that in experiment. A simple approach to experimentally investigating this phenomenon is to employ granular packings, which are naturally heterogeneous with weak constraint. The heterogeneity of granular materials arises from the randomness of their structure and the sheer quantity of discrete sub-elements. Any given particle in a granular medium might, for example, possess fewer or more than 6 contact sites with other particles—of which there are $\sim 10^{10}$ in every 1 g of shape memory powder—and be irregularly shaped. Since the granular packing is non-bonded by definition, the structure will evolve during compression, adding more complexity to the problem. As shown in Fig. 3, however, the specific manner of heterogeneity in a granular packing is still analogous to the stress concentration sites responsible for the hypothesized continuous transformation mode of composites or architectured structures.

Stress-induced martensitic transformation in granular shape memory ceramic (CeO_2-doped ZrO_2) packings has been in situ investigated by Rauch et al. [34]. Using the in situ neutron diffraction setup shown in Fig. 5A, two different compositions of CeO_2-doped ZrO_2 granular packings consisting of single-crystal particles are subjected to compression: 12-mol% CeO_2 and 15-mol% CeO_2. The 12-mol% CeO_2 particles have a metastable austenite phase such that any martensite formed during loading is not transformed back to austenite during unloading (Fig. 5B). The 15-mol% CeO_2 particles correspond to a stable austenite phase that exhibits superelastic behavior: martensite forms during loading and then is reverted back to austenite during unloading (Fig. 5C) [1, 34]. The hysteresis between the forward martensitic transformation and the reverse transformation back to austenite is due to the

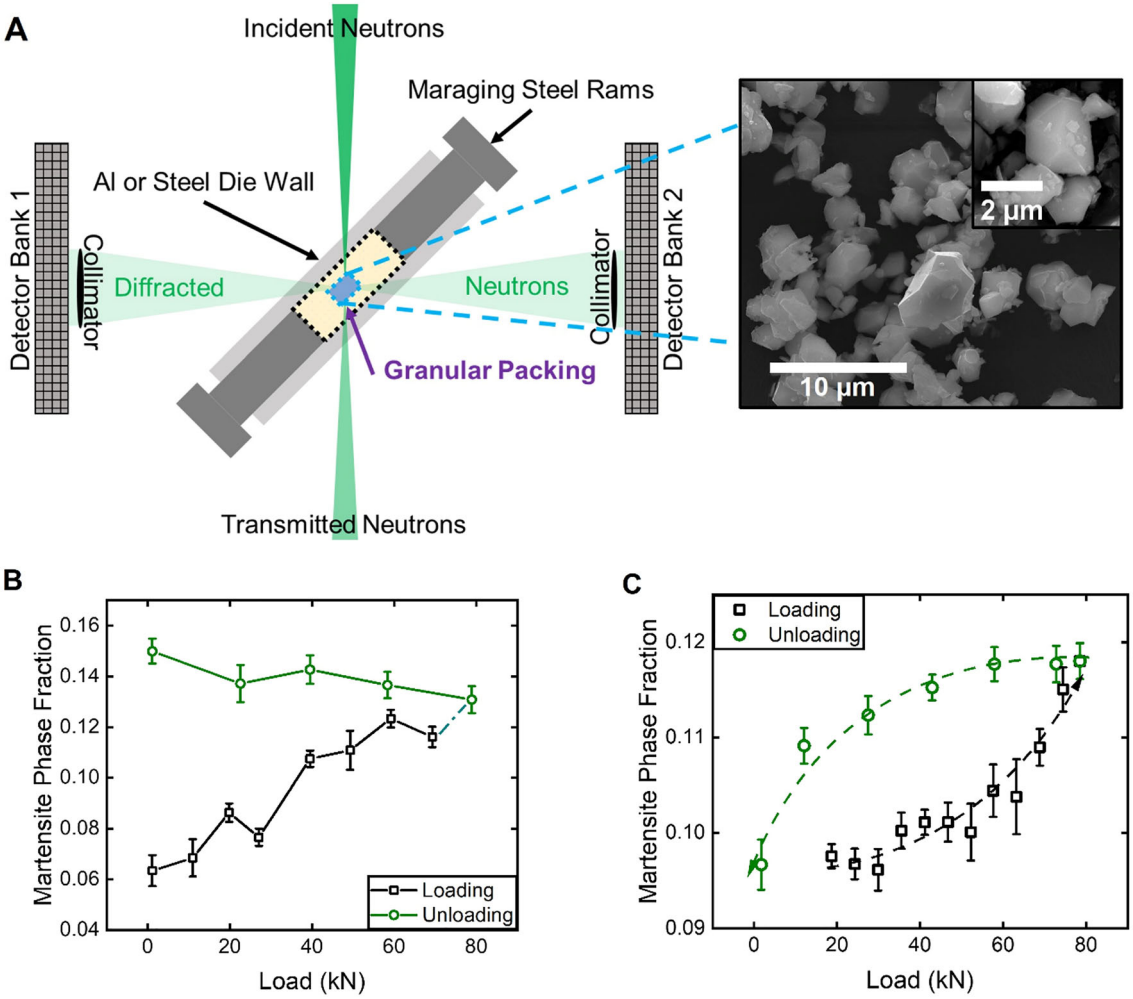

Fig. 5 **A** Arrangement for in situ neutron diffraction during loading for granular packings. Martensite content versus applied load for ZrO_2 particles with **B** 12-mol% CeO_2 and **C** 15-mol% CeO_2 [34]. Reprinted from *Acta Materialia*, Vol 168, Rauch HA, Chen Y, An K, Yu HZ, In situ investigation of stress-induced martensitic transformation in granular shape memory ceramic packings, Pages 362–375, Copyright 2019, with permission from Elsevier

lower critical stress for the reverse transformation [27]. For both compositions, the martensite nucleation occurs over a wide load range, as seen in Fig. 5B and C, due to the force chain-based mesoscale stress distribution and Hertzian contact-based microscale stress distribution, matching the expected behavior of a continuous transformation mode in Fig. 1B. In this data, there is no apparent critical stress because of the minimal mechanical constraint among particles.

The distribution of force experienced by particles in a granular packing is depicted in Fig. 6A. At any given loading condition, a majority of particles experience little or no forces aside from gravity. As the applied load on the granular packing is increased, the overall probability distribution of the force on the particles broadens, more particles experience non-zero load, and more particles exhibit loads above the critical load for the forward transformation (i.e., the load corresponding to the critical stress for that particular particle) and would thus nucleate martensite. A depiction of the resulting force chains and martensitic nucleation with increasing displacement or external load is shown in Fig. 6B. Matching the overall force distribution in Fig. 6A, the force from particle–particle contact increases with increasing displacement, so is the number of martensitic plates [34]. As the external load is then removed, the critical load for the reverse transformation to transform martensite to austenite is lower than for the forward transformation and lies to the left of the dotted line in Fig. 6A. Thus, for the same external load, the fraction of particles under a load state above the lower critical load for the reverse transformation will be greater than for the forward transformation, so the applied load must be reduced further before any martensite is reverted back to martensite, causing the hysteresis shown in Fig. 5C.

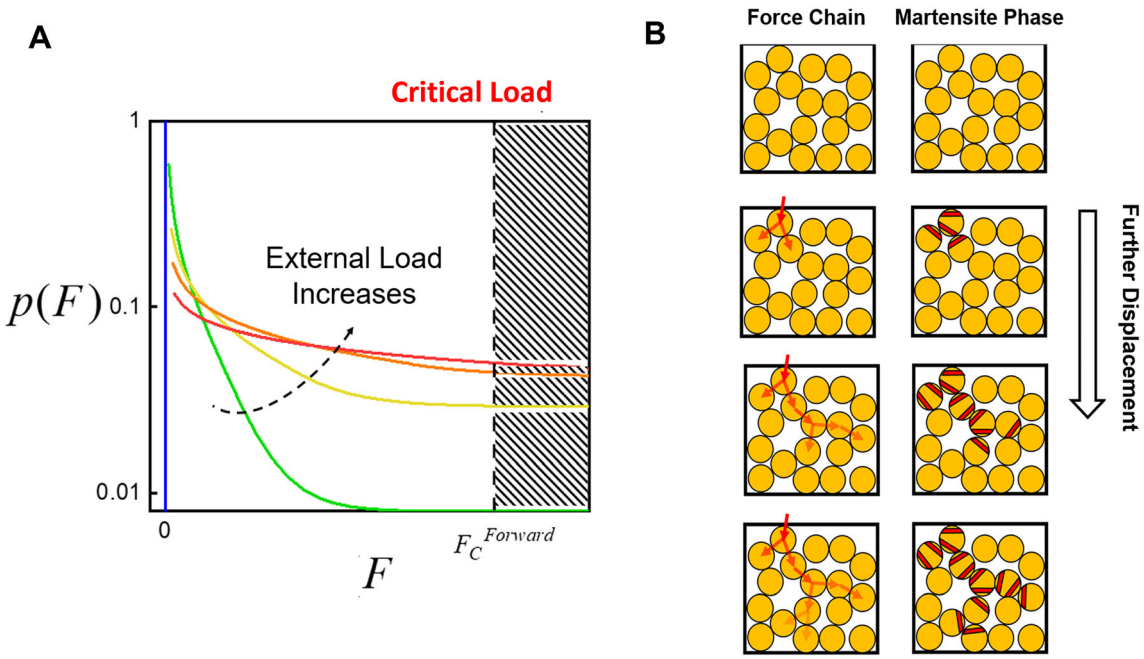

Fig. 6 **A** The probability density function of the force distribution in a granular packing and the effect of increasing load; $F_C^{Forward}$ is the critical force for martensite nucleation. **B** The force chain and martensite phase evolution in granular packing under increasing displacement [34]. Reprinted from *Acta Materialia*, Vol 168, Rauch HA, Chen Y, An K, Yu HZ, In situ investigation of stress-induced martensitic transformation in granular shape memory ceramic packings, Pages 362–375, Copyright 2019, with permission from Elsevier

Similar to granular packings, cellular architectured materials have likewise shown to form martensite preferentially due to stress concentration, as previously discussed. Recently, a slurry based on yttrium-stabilized tetragonal zirconia polycrystals (Y-TZP) has been developed for stereolithography to additively manufacture micro-honeycomb structures. Upon compression, the Y-TZP micro-honeycomb forms approximately 10-vol% martensite when it is loaded to a maximum axial stress of 270 MPa [25].

In addition to stress-induced martensitic transformation, the meso/micro-structured shape memory materials can exhibit interesting behavior in thermally induced reverse martensitic phase transformation. Figure 7A and B shows the behavior of a granular packing consisting of ZrO_2 particles and a Cu-ZrO_2 (20 vol%) composite. The former is adapted from published work in Reference [34]; the latter is part of the authors' ongoing work on solid-state additive manufacturing of metal matrix composites. In both cases, the shape memory ceramic ZrO_2 is doped with 12-mol% CeO_2. The granular packing and composite are first subjected to compression with axial compressive stresses of approximately 1000 MPa and 915 MPa, respectively. After compression, there is non-uniform distribution of the martensite phase; upon heating, thermally induced reverse martensitic transformation occurs separately among local regions due to factors such as particle morphology, size, and the dependence of A_s on the martensite concentration [33]. As a result, the martensite content gradually decreases over a very wide temperature range without a well-defined A_s or A_f. These results may be viewed as examples of continuous transformation mode in thermally induced martensitic transformation.

Note that the modeling insights and experimental evidence above are discussed in the context of shape memory ceramics, in which intergranular constraint governs the transformation characteristics. The same mesostructure and micro-structure design strategy may be applicable to some shape memory metal alloys as well, like Cu-based or NiMnGa, for which an increase of the surface area and a decrease of the triple junctions also promote martensitic transformation. For NiTi, however, the shape strain upon transformation is very small, and intergranular constraint effect is not significant. Instead, the triple junctions act as nucleation sites for martensitic transformation, resulting in a different effect on the global transformation behavior [48].

Conclusions and Future Perspectives

We have discussed how mesostructure and microstructure engineering can be leveraged to change the characteristics of thermodynamic driving force and nucleation barrier in martensitic transformation of shape memory ceramics. With heterogeneous driving force and weak mechanical

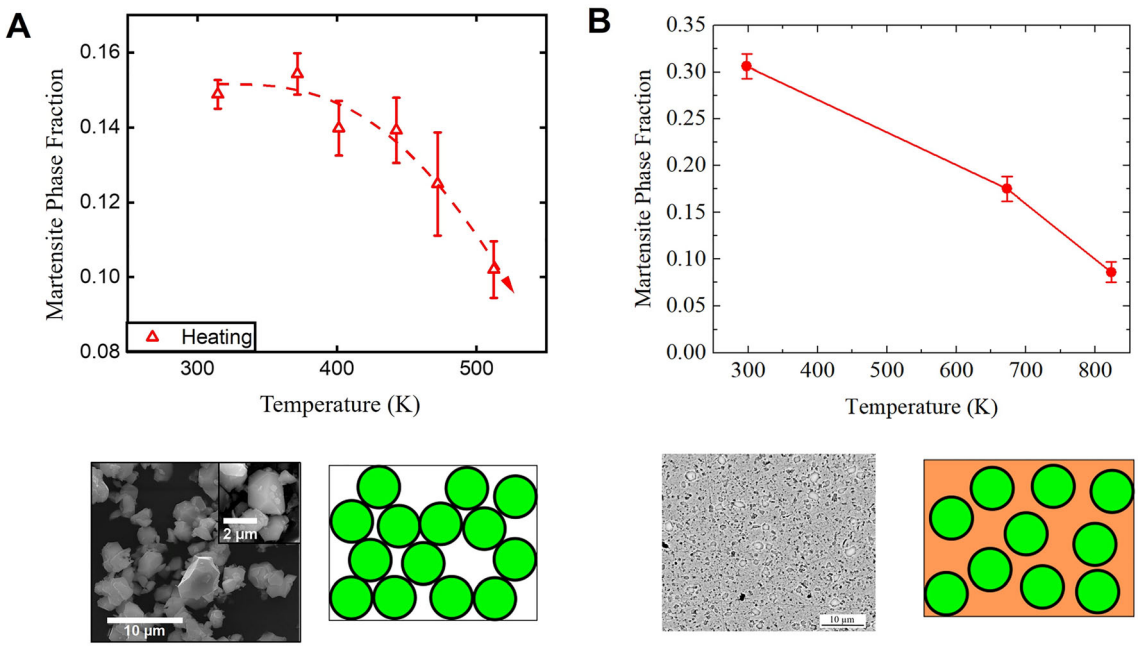

Fig. 7 Comparison of the thermally induced reverse martensitic transformation for **A** granular packings and **B** metal matrix composites, as well as SEM micrographs of their actual structures and their idealized structures [34]. **A** Reprinted from *Acta Materialia*, Vol 168, Rauch HA, Chen Y, An K, Yu HZ, In situ investigation of stress-induced martensitic transformation in granular shape memory ceramic packings, Pages 362–375, Copyright 2019, with permission from Elsevier

constraint demonstrated in granular packings, metal matrix composites, and cellular architectured materials, the martensitic transformation can occur locally and sequentially without long-range growth via autocatalysis. This is in great contrast to bulk monolithic shape memory ceramics, resulting in a globally continuous transformation mode. This new transformation mode is characterized by a continuous transformation volume change with the load or temperature; there may no longer be well-defined critical stresses or temperatures.

Using the mesostructure and microstructure design strategy, the exact relationship between the transformed volume and external stimulus can be controlled, which paves the road toward broader applications of shape memory materials, such as universal energy dissipation and continual actuation. This design strategy can be accelerated with the aid of computer modeling, thanks to which the quantitative transformation–stimulus relationship can be quickly tested and controlled via structural optimization. Practical implementation of this strategy will rely on future advances in additive manufacturing and advanced materials processing, which will allow one to create mesostructures and microstructures with desired geometries and characteristic length scales.

Acknowledgements The authors would like to acknowledge the support from the National Science Foundation (NSF) (No. CMMI-1853893). This work was performed in part at the Nanoscale Characterization and Fabrication Laboratory, which is supported by the Virginia Tech National Center for Earth and Environmental Nanotechnology Infrastructure (NanoEarth), a member of the National Nanotechnology Coordinated Infrastructure (NNCI), supported by NSF (ECCS 1542100 and ECCS 2025151).

References

1. Yu HZ, Hassani-Gangaraj M, Du ZH, Gan CL, Schuh CA (2017) Granular shape memory ceramic packings. Acta Mater 132:455–466. https://doi.org/10.1016/j.actamat.2017.04.057
2. Chowdhury P, Patriarca L, Ren G, Sehitoglu H (2016) Molecular dynamics modeling of NiTi superelasticity in presence of nano-precipitates. Int J Plast 81:152–167. https://doi.org/10.1016/j.ijplas.2016.01.011
3. Ogawa Y, Ando D, Sutou Y, Koike J (2016) A lightweight shape-memory magnesium alloy. Science 353(6297):368–370. https://doi.org/10.1126/science.aaf6524
4. Tanaka Y, Himuro Y, Kainuma R, Sutou Y, Omori T, Ishida K (2010) Ferrous polycrystalline shape-memory alloy showing huge superelasticity. Science 327(5972):1488–1490. https://doi.org/10.1126/science.1183169
5. Hofmann DC (2010) Shape memory bulk metallic glass composites. Science 329(5997):1294–1295. https://doi.org/10.1126/science.1193522
6. Xie T (2010) Tunable polymer multi-shape memory effect. Nature 464(7286):267–270. https://doi.org/10.1038/nature08863
7. Xie T (2011) Recent advances in polymer shape memory. Polymer 52(22):4985–5000. https://doi.org/10.1016/j.polymer.2011.08.003
8. Reyes-Morel PE, Cherng J-S, Chen IW (1988) Transformation plasticity of CeO_2-stabilized tetragonal zirconia polycrystals: II, pseudoelasticity and shape memory effect. J Am Ceram Soc

71(8):648–657. https://doi.org/10.1111/j.1151-2916.1988.tb06383.x
9. Wang Y, Ren X, Otsuka K (2006) Shape memory effect and superelasticity in a strain glass alloy. Phys Rev Lett 97(22):225703. https://doi.org/10.1103/PhysRevLett.97.225703
10. Casalena L, Bucsek AN, Pagan DC, Hommer GM, Bigelow GS, Obstalecki M, Noebe RD, Mills MJ, Stebner AP (2018) Structure-property relationships of a high strength superelastic NiTi–1Hf alloy. Adv Eng Mater 20(9):1800046. https://doi.org/10.1002/adem.201800046
11. Bucsek AN, Hudish GA, Bigelow GS, Noebe RD, Stebner AP (2016) Composition, compatibility, and the functional performances of ternary NiTiX high-temperature shape memory alloys. Shape Mem Superelasticity 2(1):62–79. https://doi.org/10.1007/s40830-016-0052-5
12. Schaedler TA, Carter WB (2016) Architected cellular materials. Annu Rev Mater Res 46(1):187–210. https://doi.org/10.1146/annurev-matsci-070115-031624
13. Restrepo D, Mankame ND, Zavattieri PD (2015) Phase transforming cellular materials. Extreme Mech Lett 4:52–60. https://doi.org/10.1016/j.eml.2015.08.001
14. Naebe M, Shirvanimoghaddam K (2016) Functionally graded materials: a review of fabrication and properties. Appl Mater Today 5:223–245. https://doi.org/10.1016/j.apmt.2016.10.001
15. Ashby MF, Chapter 11—Designing Hybrid Materials, Materials Selection in Mechanical Design (4th Edition), M.F. Ashby, (Ed.), Butterworth-Heinemann, 2011, p 299–340
16. Kazemi H, Vaziri A, Norato JA (2018) Topology optimization of structures made of discrete geometric components with different materials. J Mech Des. https://doi.org/10.1115/14040624
17. Yan X, Huang X, Zha Y, Xie YM (2014) Concurrent topology optimization of structures and their composite microstructures. Comput Struct 133:103–110. https://doi.org/10.1016/j.compstruc.2013.12.001
18. Asadpoure A, Tootkaboni M, Guest JK (2011) Robust topology optimization of structures with uncertainties in stiffness—Application to truss structures. Comput Struct 89(11):1131–1141. https://doi.org/10.1016/j.compstruc.2010.11.004
19. Zhao M, Qing H, Wang Y, Liang J, Zhao M, Geng Y, Liang J, Lu B (2021) Superelastic behaviors of additively manufactured porous NiTi shape memory alloys designed with Menger sponge-like fractal structures. Mater Des 200:109448. https://doi.org/10.1016/j.matdes.2021.109448
20. Wang Z (2019) Recent advances in novel metallic honeycomb structure. Compos Part B 166:731–741. https://doi.org/10.1016/j.compositesb.2019.02.011
21. Meza LR, Das S, Greer JR (2014) Strong, lightweight, and recoverable three-dimensional ceramic nanolattices. Science 345(6202):1322–1326. https://doi.org/10.1126/science.1255908
22. Cui H, Hensleigh R, Yao D, Maurya D, Kumar P, Kang MG, Priya S, Zheng XR (2019) Three-dimensional printing of piezoelectric materials with designed anisotropy and directional response. Nat Mater 18(3):234–241. https://doi.org/10.1038/s41563-018-0268-1
23. Portela CM, Edwards BW, Veysset D, Sun Y, Nelson KA, Kochmann DM, Greer JR (2021) Supersonic impact resilience of nanoarchitected carbon. Nat Mater 20(11):1491–1497. https://doi.org/10.1038/s41563-021-01033-z
24. Bauer J, Meza LR, Schaedler TA, Schwaiger R, Zheng X, Valdevit L (2017) Nanolattices: an emerging class of mechanical metamaterials. Adv Mater 29(40):1701850. https://doi.org/10.1002/adma.201701850
25. Rauch HA, Cui H, Knight KP, Griffiths RJ, Yoder JK, Zheng X, Yu HZ (2022) Additive manufacturing of yttrium-stabilized tetragonal zirconia: progressive wall collapse, martensitic transformation, and energy dissipation in micro-honeycombs. Addit Manuf. https://doi.org/10.1016/j.addma.2022.102692
26. Machado G, Louche H, Alonso T, Favier D (2015) Superelastic cellular NiTi tube-based materials: Fabrication, experiments and modeling. Mater Des (1980–2015) 65:212–220. https://doi.org/10.1016/j.matdes.2014.09.007
27. Du Z, Zeng XM, Liu Q, Schuh CA, Gan CL (2016) Superelasticity in micro-scale shape memory ceramic particles. Acta Mater 123:255–263
28. Lai A, Du Z, Gan CL, Schuh CA (2013) Shape memory and superelastic ceramics at small scales. Science 341(6153):1505–1508. https://doi.org/10.1126/science.1239745
29. Chen Y, Schuh CA (2011) Size effects in shape memory alloy microwires. Acta Mater 59(2):537–553. https://doi.org/10.1016/j.actamat.2010.09.057
30. Dunand DC, Müllner P (2011) Size effects on magnetic actuation in Ni-Mn-Ga shape-memory alloys. Adv Mater 23(2):216–232. https://doi.org/10.1002/adma.201002753
31. Zhu J, Gao Y, Wang D, Zhang T-Y, Wang Y (2017) Taming martensitic transformation via concentration modulation at nanoscale. Acta Mater 130:196–207. https://doi.org/10.1016/j.actamat.2017.03.042
32. Wang D, Hou S, Wang Y, Ding X, Ren S, Ren X, Wang Y (2014) Superelasticity of slim hysteresis over a wide temperature range by nanodomains of martensite. Acta Mater 66:349–359. https://doi.org/10.1016/j.actamat.2013.11.022
33. Rauch HA, Yu HZ (2020) Effects of mechanical constraint on thermally induced reverse martensitic transformation in granular shape memory ceramic packings. J Appl Phys 128(24):245102. https://doi.org/10.1063/5.0035041
34. Rauch HA, Chen Y, An K, Yu HZ (2019) In situ investigation of stress-induced martensitic transformation in granular shape memory ceramic packings. Acta Mater 168:362–375. https://doi.org/10.1016/j.actamat.2019.02.028
35. Majmudar TS, Behringer RP (2005) Contact force measurements and stress-induced anisotropy in granular materials. Nature 435(7045):1079–1082. https://doi.org/10.1038/nature03805
36. Tordesillas A, Tobin ST, Cil M, Alshibli K, Behringer RP (2015) Network flow model of force transmission in unbonded and bonded granular media. Phys Rev E 91(6):062204. https://doi.org/10.1103/PhysRevE.91.062204
37. Boyd JG, Lagoudas DC (1996) A thermodynamical constitutive model for shape memory materials. Part I. The monolithic shape memory alloy. Int J Plast 12(6):805–842. https://doi.org/10.1016/S0749-6419(96)00030-7
38. COMSOL Structural Mechanics Module User's Guide, 2020
39. Shape Memory Alloys: Modeling and Engineering Applications, D.C. Lagoudas, (Ed.), Springer, 2008
40. Lagoudas DC, Entchev PB (2004) Modeling of transformation-induced plasticity and its effect on the behavior of porous shape memory alloys. Part I: constitutive model for fully dense SMAs. Mech Mater 36(9):865–892. https://doi.org/10.1016/j.mechmat.2003.08.006
41. Lagoudas DC, Entchev PB, Popov P, Patoor E, Brinson LC, Gao XJ (2006) Shape memory alloys, Part II: Modeling of polycrystals. Mech Mater 38(5–6):430–462. https://doi.org/10.1016/j.mechmat.2005.08.003
42. Reyes-Morel PE, Chen I-W (1988) Transformation plasticity of CeO_2-Stabilized tetragonal zirconia polycrystals: I, stress assistance and autocatalysis. J Am Ceram Soc 71(5):343–353. https://doi.org/10.1111/j.1151-2916.1988.tb05052.x
43. Du Z, Zeng XM, Liu Q, Lai A, Amini S, Miserez A, Schuh CA, Gan CL (2015) Size effects and shape memory properties in ZrO_2 ceramic micro- and nano-pillars. Scripta Mater 101:40–43. https://doi.org/10.1016/j.scriptamat.2015.01.013

44. Maran S, Masters IG, Gibbons GJ (2020) Additive manufacture of 3D auxetic structures by laser powder bed fusion—Design influence on manufacturing accuracy and mechanical properties. Appl Sci. https://doi.org/10.3390/app10217738
45. Arghavani J, Auricchio F, Naghdabadi R, Reali A, Sohrabpour S (2010) A 3-D phenomenological constitutive model for shape memory alloys under multiaxial loadings. Int J Plast 26(7):976–991. https://doi.org/10.1016/j.ijplas.2009.12.003
46. Auricchio F (2001) A robust integration-algorithm for a finite-strain shape-memory-alloy superelastic model. Int J Plast 17(7):971–990. https://doi.org/10.1016/S0749-6419(00)00050-4
47. Auricchio F, Petrini L (2004) A three-dimensional model describing stress-temperature induced solid phase transformations: solution algorithm and boundary value problems. Int J Numer Methods Eng 61(6):807–836. https://doi.org/10.1002/nme.1086
48. Ahadi A, Sun Q (2014) Effects of grain size on the rate-dependent thermomechanical responses of nanostructured superelastic NiTi. Acta Mater 76(2014):186–197